EXTENDED SCALING METHOD FOR NONSIMILARITY IN REYNOLDS NUMBER, STAGGER ANGLE AND BLADE NUMBER

Sebastian SAUL, Peter F. PELZ

Technische Universität Darmstadt, Chair of Fluid Systems,
Otto-Berndt-Straße 2, 64287 Darmstadt, Germany

SUMMARY

Acceptance tests for large turbomachines are carried out with the help of small-scaled models on standardized test rigs. This non-similarity, e.g. in Reynolds and Mach number between model and prototype causes an efficiency change. Therefore, the prediction of efficiency change is done by scaling methods. *Darmstadt Scaling Method* is extended to consider different stagger angles and different blade numbers for axial fans. The method is validated with experimental data and shows good agreements in the stagger angle range from $-18°$ to $+12°$ and Reynolds number ranges of $Re = 2.2\text{E}6 \ldots 6.5\text{E}6$ for half- and full-equipped rotors with respect to blade number.

NOMENCLATURE

Latin symbols

a	speed of sound	m	exponent	t	pitch
A	wetted surface	Ma	Mach number	T	temperature
c	absolute velocity	$\dot{m}$	mass flow rate	u	circumferential velocity
c_f	friction coefficient	n	proportional factor	V	loss factor
D	diameter	p	pressure	$\dot{V}$	volume flow rate
f	shape factor	P	power	w	relative velocity
i	incidence angle	R	gas constant	Y	specific work
k	roughness	Re	Reynolds number	z	number of blades
l	length	s	gap		

Greek symbols

β	angle	η	efficiency	ϱ	density
γ	isentropic exponent	κ	scaling factor	σ	specific speed

γ_R	stagger angle	λ	power coefficient	φ	flow coefficient
ε	inefficiency	μ	kinematic viscosity	ϕ	deflection
ζ	loss coefficient	ν	hub-to-tip ratio	ψ	pressure coefficient

Indices

+	dimensionless	BEP	best efficiency point	m	mean
*	local point or reference	f	friction	o	outer
1	rotor inlet	i	inner	R	rotor
2	rotor outlet	Inc	incidence	S	stator / shaft
3	inlet stator	l	loss		

INTRODUCTION

Acceptance tests for large turbomachines, like fans in wind tunnels, mines or power plants with impeller diameters $D_o > 2$ m, are carried out on standardized model test rigs due to better accessibility and lower measuring uncertainty. Fan models are downscaled to a good handling size to lower efforts and manufacturing and operating costs [1]. Today, rapid prototyped models with impeller diameters up to $D_o \approx 0.4$ m become more and more attractive for testing purposes due to fast manufactured and high quality models.

The efficiency η depends on the type, dimensionless size, quality and operating point of the fan

$$\eta = \eta(TYPE, DIMENSIONLESS\ SIZE, QUALITY, OPERATING\ POINT) \quad (1)$$

and can be described by independent dimensionless products. The type of the fan considers the shape and is determined by the specific speed σ. The Reynolds number Re and the Mach number Ma characterize the dimensionless size. The quality of the fan is measured by the relative roughness k_+ and relative gap s_+. The flow coefficient φ describes the operating point.

For non-similarity the efficiency of a prototype is given by

$$\eta = \eta'(\sigma' = \sigma, Re', Ma', k'_+, s'_+, \varphi' = \varphi) + \Delta\eta(\sigma, Re, Re', Ma, Ma', k_+, k'_+, s_+, s'_+, \varphi), \quad (2)$$

with the unknown efficiency difference $\Delta\eta$. As the following section explains in detail, in most cases full similarity is not achievable and so-called *scaling methods* determine the efficiency change [2, 3]. To be considered reliable, scaling methods must be physically based. It is deemed valuable, if the uncertainty of the scaling $\delta(\Delta\eta)$ plus the model measurement uncertainty $\delta\eta'$ is smaller than an in situ measurement of the prototype $\delta\eta$

$$\delta\eta > \delta\eta' + \delta(\Delta\eta). \quad (3)$$

To be universally applicable, an efficiency scaling method for fans must be valid in a wide range of specific speeds σ, which includes axial and centrifugal fans. Unfortunately, the given scaling methods are either unreliable, not valuable or specific.

The most common scaling method by Ackeret [2] is an empirically based method. Ackeret's method, which is given by

$$\frac{1-\eta}{1-\eta'} = 1 - V + V\left(\frac{Re}{Re'}\right)^m, \quad (4)$$

depends on the Reynolds number Re, an empirical exponent m and the loss fraction V. The conversion of eq. (4) yields Ackeret's efficiency change

$$\Delta\eta_{\text{Ackeret}} = (1-\eta')\,V\left[1-\left(\frac{Re}{Re'}\right)^{m}\right]. \tag{5}$$

Ackeret assumes a loss fraction of $V = 0.5$, which means, that 50 % of all losses are scalable. The exponent $m = -0.2$ indicates an assumed hydraulically smooth surface. According to the ISO 13348:2007 (section 7.1.5.2) [4], the exponent m is positive instead of negative. Hence, scale-up and -down are mixed up.

In a real turbomachine, both parameters, loss fraction V and exponent m, depend on the type of the turbomachine. Wiesner [5] summarizes several works which investigate axial and centrifugal compressors, pumps and turbines. The exponent varies in the range of $m = -0.2 \ldots -0.1$ for most turbomachines and the loss fraction varies between $V = 0.5 \ldots 1$. This scattering of input parameters V and m results in higher scaling uncertainties. Hence, the ISO 13348 [4] recommends only half of Ackeret's predicted efficiency change, due to assumed constant loss fraction $V = 0.5$ and exponent $m = -0.2$. Thus, there is a need for a reliable determination of efficiency change $\Delta\eta$.

This paper bases on a reliable, valuable and universal scaling method, which is extended to determine the efficiency change $\Delta\eta$ dependent on the incidence angle between flow and rotor blades i. The presented method is validated for axial fans with different numbers of rotor blades and stagger angles.

The paper is organized as follows. The next section contains the similarity theory, followed by the introduction of *Darmstadt Scaling Method*. Hereafter, the experimental validation is presented and the experimental results as well as the validation of *Darmstadt Scaling Method* are discussed. Finally, the paper closes with a summary and a conclusion.

SIMILARITY THEORY

Model and prototype only show the same function, i.e. dependent dimensionless products, pressure coefficient $\psi := 2Y/u_\mathrm{o}^2 = \psi(\sigma, Re, Ma, k_+, s_+, \varphi)$ (a definition is indicated by $:=$) and efficiency $\eta := Y\dot{m}/P_\mathrm{S} = \eta\,(\sigma, Re, Ma, k_+, s_+, \varphi)$ (specific work Y, circumferential velocity u_o, mass flow rate $\dot{m}$, shaft power P_S), if all independent dimensionless products remain unchanged. The independent dimensionless products are summarized below. The subscript 1 denotes the inlet of the fan and the subscript o denotes the outer area at the casing:

- specific speed $\sigma := \varphi^{1/2}\,\psi^{-3/4}$,
- Reynolds number $Re := D_\mathrm{o} u_\mathrm{o} \varrho_1/\mu_1$ (dynamic viscosity μ_1, density ϱ_1),
- Mach number $Ma := u_\mathrm{o}/a_1$ (speed of sound $a_1 = \sqrt{\gamma R T_1}$, isentropic exponent γ, gas constant R, temperature T_1),
- relative roughness $k_+ := k/D_\mathrm{o}$ (absolute roughness k),
- relative gap $s_+ := s/D_\mathrm{o}$ (absolute gap s) and
- flow coefficient $\varphi := 4\dot{V}_1/(\pi D_\mathrm{o}^2 u_\mathrm{o})$ (volume flow rate $\dot{V}_1$).

The geometrical similarity is preserved, if all geometric measures of the machine are scaled with the same scaling factor $\kappa := D_\mathrm{o}'/D_\mathrm{o}$, being the ratio of the impeller diameter of the model, which is indicated by a prime ($'$), to the prototype. This includes the roughness $k' = \kappa\, k$ and the gap $s' = \kappa\, s$. Besides the geometrical similarity, a full physical similarity (hence $\eta = \eta'$, $\psi = \psi'$) is only reached, if $Re = Re'$ and $Ma = Ma'$ is also ensured. For practical reasons, the geometrical similarity is never fully achieved. The absolute surface roughness k and gap s are often not scalable [1], due to the manufacturing process. Furthermore, the Reynolds number Re cannot be preserved because the power consumption of model measurements would increase unphysically high [6]. The mentioned non-similarity results in different efficiencies of model and prototype $\eta' \neq \eta$. Therefore, there is a need to describe the efficiency change $\Delta\eta = \eta - \eta'$.

DARMSTADT SCALING METHOD

The extended scaling method is based on the inefficiency, defined as the complementary of the efficiency $\varepsilon \coloneqq 1 - \eta$ [7, 8, 9]. According to Pelz & Stonjek [9], the difference of inefficiency is

$$\Delta\varepsilon = \varepsilon \frac{\Delta\zeta}{\zeta} + \mathcal{O}(\varepsilon^2), \tag{6}$$

with the dimensionless losses inside the machine $\zeta \coloneqq 2Y_\mathrm{I}/u_\mathrm{o}^2$ (with the loss of specific Y_I) and the difference of losses from model to prototype $\Delta\zeta = \zeta' - \zeta$. For the introduction of the incidence losses, the scaling method is used for constant gap losses and the focus is on the efficiency scaling of the best efficiency point $\eta = \eta_\mathrm{BEP}$. Hence, the scaling method yields

$$\Delta\eta_\mathrm{DARMSTADT} = (\eta - \eta')_\mathrm{BEP} = (1 - \eta')\frac{\zeta' - \zeta}{\zeta'}. \tag{7}$$

The efficiency of the model η' is measured on standardized test rigs. The assumed overall loss coefficients ζ of the turbomachine consists of the friction losses in the rotor, stator ($\zeta_\mathrm{f,R}$ and $\zeta_\mathrm{f,S}$) and the incidence losses ζ_Inc. According to Froude's hypothesis [10], the losses are independent of each other and the overall loss is a summation of all independent losses

$$\zeta = \zeta_\mathrm{f,R} + \zeta_\mathrm{f,S} + \zeta_\mathrm{Inc}. \tag{8}$$

All loss sources have to be considered in an appropriate way. By doing so, shape factors f_i are introduced and eq. (8) yields

$$\zeta = \zeta_\mathrm{f,R} + \zeta_\mathrm{f,S} + \zeta_\mathrm{Inc} = c^*_\mathrm{f,R}\, f_\mathrm{f,R} + c^*_\mathrm{f,S}\, f_\mathrm{f,S} + \zeta^*_\mathrm{Inc}\, f_\mathrm{Inc}, \tag{9}$$

with the local friction loss coefficient for the rotor, stator ($c^*_\mathrm{f,R}$ and $c^*_\mathrm{f,S}$) and the local loss coefficient for the incidence loss (ζ^*_Inc). All local loss coefficients are marked with an asterisk (*). The remaining ones refer to the machine.

Friction losses

The friction losses in the rotor $c^*_\mathrm{f,R} = c^*_\mathrm{f,R}(Re^*_\mathrm{R}, k_{+,\mathrm{R}})$ and the stator $c^*_\mathrm{f,S} = c^*_\mathrm{f,S}(Re^*_\mathrm{S}, k_{+,\mathrm{S}})$ are modelled as a flat plate and are depended on the local Reynolds number Re^* and the relative roughness k_+.

A turbulent flow is assumed and Gülich's approximation [11] for the friction coefficient for hydraulically smooth and rough flows is

$$c_\mathrm{f} = \frac{0.136}{\left[-\log_{10}\left(0.2\, k_+ + \frac{12.5}{Re^*}\right)\right]^{2.15}}. \tag{10}$$

The relative roughness is defined as $k_+ = k/l$, with the absolute roughness in the rotor k_R or in the stator k_S and the chord length in the mean section of the rotor blade l_R or stator blade l_S. The local Reynolds number in the rotor yields

$$Re^*_\mathrm{R} = \frac{\bar{w}}{u_\mathrm{o}}\frac{l_\mathrm{R}}{D_\mathrm{o}} Re, \tag{11}$$

with the average relative velocity in the rotor and at mean section $\bar{w} = (w_1 + w_2)/2$. The inlet velocity of the rotor is given by

$$w_1 = u_\mathrm{o}\sqrt{\frac{(1+\nu)^2}{4} + \frac{\varphi^2}{(1-\nu^2)^2}} \tag{12}$$

and the outlet velocity of the rotor is

$$w_2 = u_\mathrm{o}\sqrt{\frac{\varphi^2}{(1-\nu^2)^2} + \left(\frac{1+\nu}{2} - \frac{\lambda}{\varphi + \varphi\nu}\right)^2}, \tag{13}$$

with the hub-to-tip ratio ν and the power coefficient $\lambda \coloneqq 8P_\mathrm{S}/(\pi\varrho D_\mathrm{o}^2 u_\mathrm{o}^3)$.

The Reynolds number in the stator is calculated with a similar transformation yielding to

$$Re_\mathrm{S}^* = \frac{\bar{c}}{u_\mathrm{o}}\frac{l_\mathrm{S}}{D_\mathrm{o}}Re, \tag{14}$$

with the average absolute velocity and at the mean section in the stator $\bar{c} = (c_3 + c_4)/2$. The inlet velocity of the stator is

$$c_3 = u_\mathrm{o}\sqrt{\frac{\varphi^2}{(1-\nu^2)^2} + \left(\frac{\lambda}{\varphi + \varphi\nu}\right)^2} \tag{15}$$

and the outlet velocity is given by

$$c_4 = u_\mathrm{o}\frac{\varphi}{1-\nu^2}.$$

Incidence losses

Figure 1 shows the flow through a cascade of flat and thin plates. Thoma [12] derives the loss coefficient for the incidence loss of such a cascade of flat and thin plates. With the help of the balance of momentum in $\vec{e}_x$- and $\vec{e}_y$-direction, Bernoulli's equation and an assumed negligible wall friction, the loss coefficient yields

$$\zeta_\mathrm{Inc}^* \coloneqq \frac{2\Delta p_\mathrm{l}}{\varrho_1 c_1^2} = \tan^2(\Delta\beta_\mathrm{Inc}), \tag{16}$$

with the pressure loss in the cascade Δp_l, the density ϱ_1 and the incoming velocity c_1. The real incidence is $\Delta\beta_\mathrm{Inc}$. This model is valid for an incompressible flow. For axial fans, a low Mach number is assumed but it is expandable for compressible flows as well. Saul et al. [13] derive a model for a compressible flow through a cascade of plates.

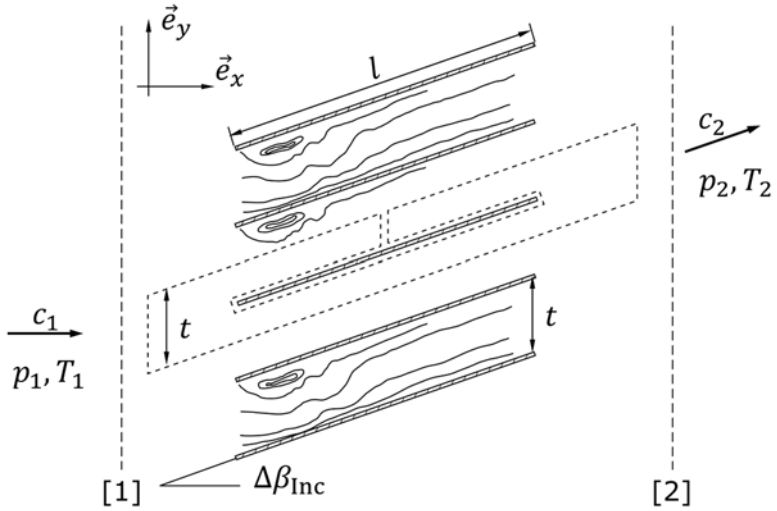

Figure 1: Schematic flow through a cascade of flat and thin plates [13].

For axial fan purposes, the incidence angle $\Delta\beta_{\mathrm{Inc}}$ is calculated at the mean diameter of the rotor. For better results, fan design parameters shall be taken into account, because the incidence angle of an airfoil depends on the stagger angle γ_{R} and the axial solidity. According to Carolus [14], the relation between real incidence angle $\Delta\beta^*_{\mathrm{Inc}}$ and geometrical incidence angle $\Delta\beta_{\mathrm{Inc}}$ between profile and inflow yields

$$\Delta\beta^*_{\mathrm{Inc}} = \Delta\beta_{\mathrm{Inc}} - i_0 - n\phi - (i_c - i_{2\mathrm{D}}), \tag{17}$$

with the design incidence angle of a symmetric profile i_0, the proportional factor n, the deflection $\phi = \beta_{\mathrm{R2}} - \beta_{\mathrm{R1}}$ (with the blade inlet and outlet angles β_{R1} and β_{R2}) and correction term for three-dimensional effects which is in the mean section $(i_c - i_{2\mathrm{D}}) = -1°$. All these parameters are explained by Carolus [14] and base on Lieblein's experimental investigations [15]. The geometrical incidence angle is given by

$$\Delta\beta_{\mathrm{Inc}} = \beta_{\mathrm{R1}} - \beta_1, \tag{18}$$

with the blade inlet angle β_{R1} and the flow inlet angle β_1 in the mean section. Figure 2 shows the angles and the velocity triangle at rotor inlet. The flow inlet angle in the mean section yields

$$\beta_1 = \arctan\left[\frac{2\varphi}{(1-\nu^2)(1+\nu)}\right]. \tag{19}$$

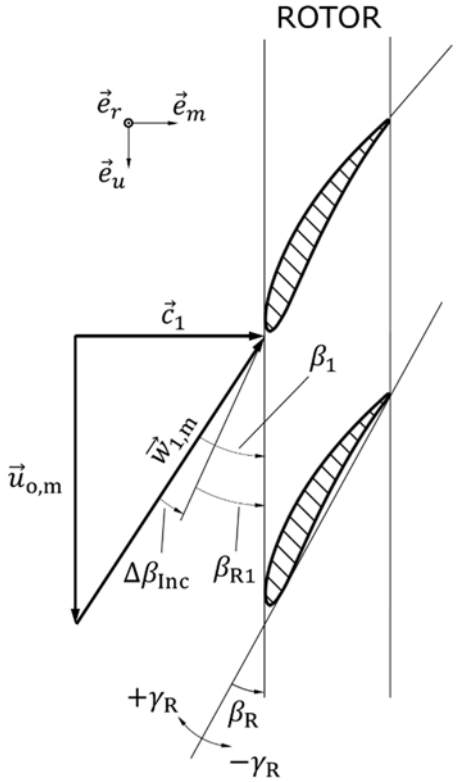

Figure 2: Velocity triangle at the rotor inlet.

Shape factors

All loss coefficients are described with local length scales and velocities. Thus, a transformation from the local reference to a global reference is necessary. This transformation is done by shape factors. All loss coefficients and shape factors are physically based and only depend on the geometry and the operating point (Stonjek [7] and Saul [16]).

The shape factor for the friction coefficient in the rotor [7] is

$$f_{\mathrm{R}} = \frac{4A_{\mathrm{R}}}{D_{\mathrm{o}}^2\pi}\left(\frac{\bar{w}_{\mathrm{R}}}{u_{\mathrm{o}}}\right)^3 \frac{1}{\varphi}, \tag{20}$$

with the wetted surface of the rotor A_{R}, the average relative velocity in the rotor in the mean section $\bar{w}_{\mathrm{R}}$ and the flow coefficient at best efficiency point φ. The wetted surface A_{R} depends on the geometry and the average velocity $\bar{w}_{\mathrm{R}}$ depends on the geometry and the operating point. Geometry and operating point are known for model and prototype. All shape factors are the same for model and prototype, $f_i = f_i'$.

According to eq. (17), the shape factor for the friction coefficient in the stator yields

$$f_{\mathrm{S}} = \frac{4A_{\mathrm{S}}}{D_{\mathrm{o}}^2\pi}\left(\frac{\bar{c}_{\mathrm{S}}}{u_{\mathrm{o}}}\right)^3 \frac{1}{\varphi}, \tag{21}$$

with the wetted surface of the stator A_{S} and the average absolute velocity in the stator $\bar{c}_{\mathrm{S}}$.

The shape factor for the incidence loss [16] is

$$f_{\mathrm{Inc}} = \frac{1-\nu^2}{\varphi}\left(\frac{w_1}{u_{\mathrm{o}}}\right)^3 = \frac{1-\nu^2}{\varphi}\left[\frac{(1+\nu)^2}{4} + \frac{\varphi^2}{(1-\nu^2)^2}\right]^{3/2}, \tag{22}$$

with the relative inlet velocity w_1. Eq. (19) is valid for an incoming flow with negligible angular momentum. For this case, the shape factor depends only on the flow coefficient φ, the hub-to-shroud ratio ν and the blade angle β_1.

EXPERIMENTAL VALIDATION & DISCUSSION

The validation is done with efficiency characteristics measured on standardized test rigs. First, the experimental setup is explained, followed by the measuring results and the application of the extended *Darmstadt Scaling Method*.

Experimental setup

Figure 3 shows the test rig for axial fans which is designed according to DIN 24163 [17]. The flow goes from left to right. The volume flow rate nozzle (I) is calibrated (II) to lower the measurement uncertainty. The auxiliary fan (V) in combination with the throttle (VI) allows measurements of the test fan at part- and overload conditions. A torquemeter (X) between bearings and rotor measures the aerodynamic torque transferred to the rotor without generating additional losses in the bearings. The rotor has adjustable blades to change the stagger angle. Additionally, the number of blades (see Table 1) are reducible. Therefore, the different fan types in the specific speed range of $\sigma = 0.95 \ldots 1.3$ are examinable.

Every test fan setting is investigated at five different rotational speeds, which allows measurements in the Reynolds number range of $Re = 2.2 \ldots . 6.5$ E6.

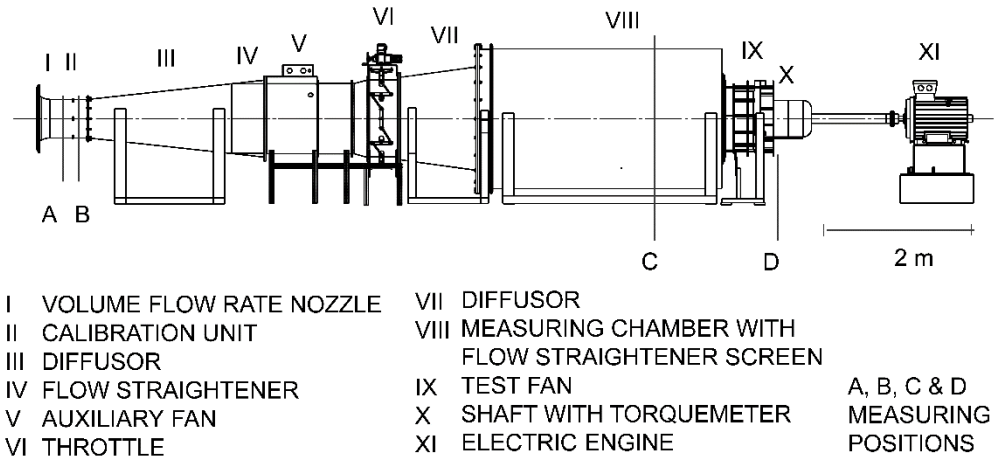

Figure 3: Axial fan test rig.

Table 1: Fan geometry and operating conditions.

term	symbol	value
specific speed	σ	$0.95 \ldots 1.05 \mid 1.2 \ldots 1.35$
hub-to-shroud ratio	$\nu = D_\mathrm{i}/D_\mathrm{o}$	0.625
outer diameter [1]	D_o	800 mm
blading		full- | half-equipped
rotor blades	z_R	$12 \mid 6$
stator blades	z_S	13
stagger angle (rotor)	γ_R	$-18° : 6° : +12°$
rel. roughness rotor	$k_{+,\mathrm{R}}$	$5.6\mathrm{E}-6$
rel. roughness stator	$k_{+,\mathrm{S}}$	$19.5\mathrm{E}-6$
rel. gap	s_+	1 ‰
Reynolds number	$Re \coloneqq \frac{u_\mathrm{o} D_\mathrm{o}}{\nu}$	$(2.2, 3.1, 4.3, 5.4, 6.5)$ E6
Mach number	$Ma \coloneqq \frac{u_\mathrm{o}}{a}$	$0.12, 0.17, 0.24, 0.3, 0.36$

Results

Figure 4 shows the efficiency and flow coefficient at the best point for all stagger angles as well as for half- and full- equipped rotor. The efficiency scaling potential depends on the stagger angle and number of blades. At a stagger angle of $\gamma_\mathrm{R} = -18°$, the efficiency rises from lowest to highest Reynolds number of $\Delta\eta \approx 5.5$ % and for a stagger angle of $\gamma_\mathrm{R} = +12°$, the efficiency rise is $\Delta\eta \approx 3$ %.

[1] The outer diameter is measured at the casing.

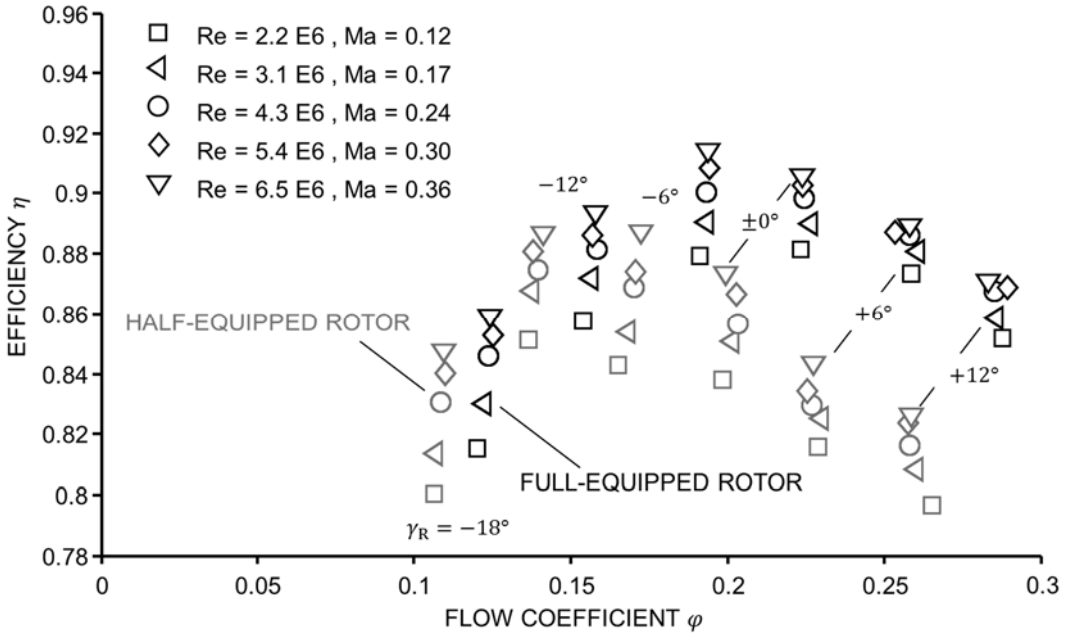

Figure 4: Summarized best efficiency points depending on stagger angle, number of rotor blades and Reynolds numbers for all investigated fan versions.

Efficiency scaling

For better comparison, the scaling method is shown with and without the consideration of the incidence loss. According to the ISO 13348 [4] only 50 % of Ackeret's efficiency change is recommended, which serves as a reference method. Figure 5 shows the maximum efficiency η with the measurement uncertainty versus the Reynolds number Re for all stagger angles γ_R and for half- and full-equipped version ($z_R = 6$ and $= 12$). A red line indicates the *Darmstadt Scaling Method* with incidence loss and without the incidence loss; a red dashed line is used.

Figure 5 compares *Darmstadt Scaling Method* with Ackeret's method and the actual measurement data. For all fan versions, *Darmstadt Scaling Method* predicts higher efficiency changes than Ackeret without overestimating the efficiency in the given Reynolds number range. In the range of stagger angles $\gamma_R = -12° \ldots 0°$, the incidence angle is low. Thus, the deviation of the predicted efficiency between the *Darmstadt Scaling Method* with and without incidence loss is low, too. At high positive stagger angles, the incidence loss increases and causes a lower efficiency change. Especially for the full-equipped version, the incidence loss consideration prevents an efficiency overestimation.

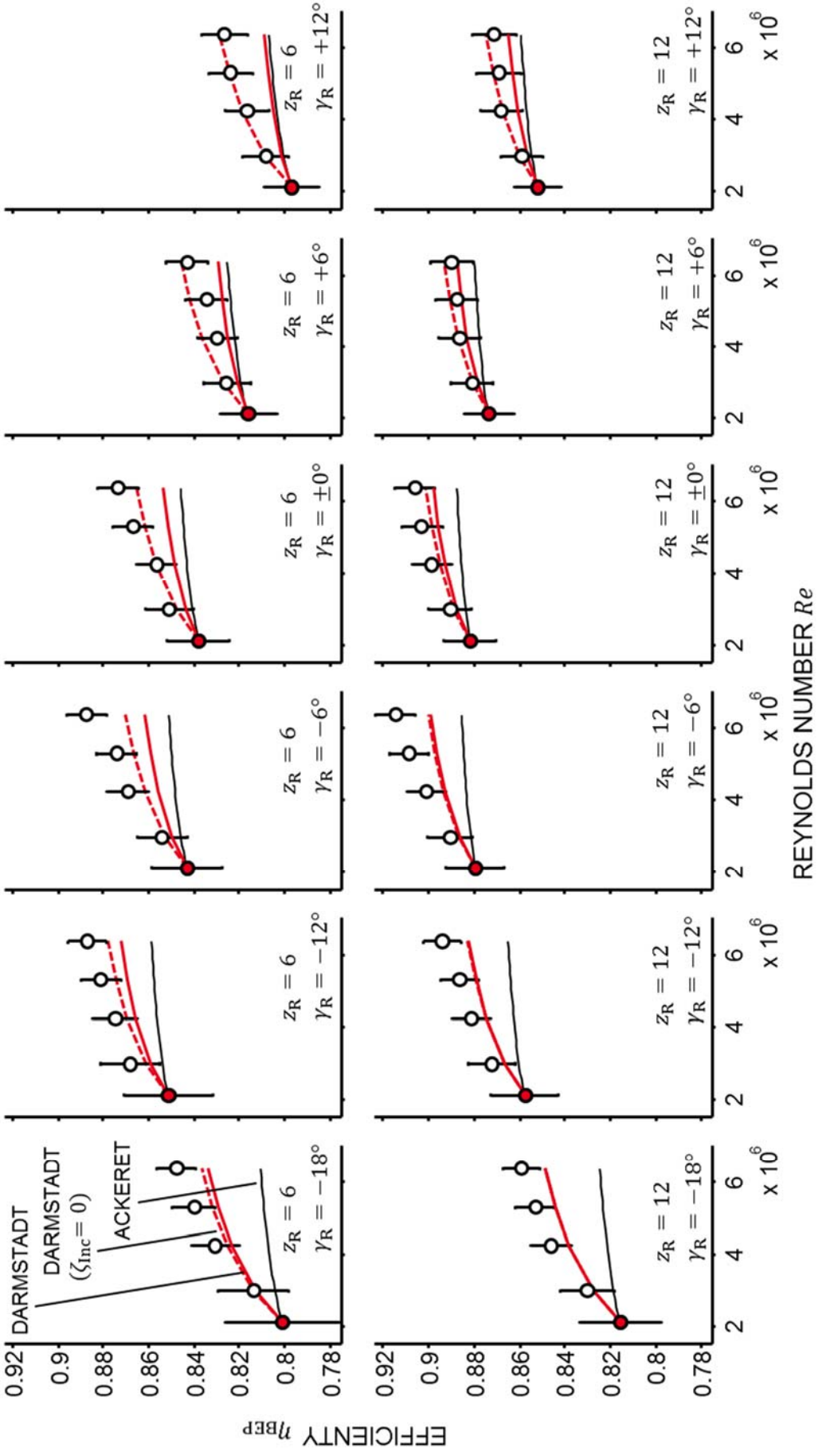

Figure 5: Darmstadt Scaling Method in comparison to Ackeret's method and measurement data. The Mach number varies between $Ma = 0.12 \ldots 0.36$ and the specific speed is in the range of $\sigma = 0.95 \ldots 1.35$.

CONCLUSION

This paper presents an extended scaling method for the efficiency of axial fans. It is validated by experimental investigations of an axial fan with different stagger angles and number of rotor blades in the Reynolds number range of $Re = 2.2\text{E}6 \ldots 6.5\text{E}6$. The experimental investigation show plausible efficiency changes depending on stagger angles, number of blades and Reynolds numbers. The efficiency potential due to increasing Reynolds numbers, varies with the stagger angle. This shows the need for a physically based scaling method, which considers different flow situations. The extended *Darmstadt Scaling Method* shows good results especially for the full-equipped fan version. The physically based shape factors and the incidence loss at the rotor inlet consider different stagger angles and numbers of rotor blades. A change of stagger angle and the number of rotor blades is a common method to match standard fans to a given system. Therefore, this is a common application example for model testing and utilized scaling method.

A good scaling method shall be reliable, valuable and universal. The extended scaling method is reliable due to its physical base. Hence, additional loss sources can be added, e.g. incidence losses. The application of the incidence loss shows a non-negligible influence on the efficiency prediction. The extended scaling method is valuable because the validation of the efficiency prediction is better than the most common scaling method from Ackeret. *Darmstadt Scaling Method* is like an assembly kit, allowing the addition of all important losses of a fan independent of the fan type, i.e. specific speed σ.

ACKNOWLEDGEMENT

The author would like to thank the Arbeitsgemeinschaft industrieller Forschungsvereinigungen Otto von Guericke e.V. (AiF), the Bundesministerium für Wirtschaft und Technologie (BMWi) and the Forschungsvereinigung für Luft- und Trocknungstechnik (FLT) e.V whose support made this work possible.

BIBLIOGRAPHY

[1] K. O. Felsch, *Die Voraussage des Betriebsverhaltens von Strömungsmaschinen aufgrund von Modellversuchen*, Maschinenmarkt, pp. 19-30, **1963**.

[2] E. Mühlemann, *Zur Aufwertung des Wirkungsgrades von Überdruck-Wasserturbinen*, Schweizerische Bauzeitung 66. Jahrg., **1948**.

[3] P. Pelz and S. Stonjek, *Introduction of an universal scale-up method for the efficiency*, in ASME Turbo Expo 2014, Düsseldorf, **2014**.

[4] ISO 13348:2007(E), *Industrial fans - Tolerances, methods of conversion and technical data presentation*, ISO, **2007**.

[5] F. J. Wiesner, *A new appraisal of Reynolds number effects on centrifugal compressor performance*, J. Eng. Gas Turbines Power, pp. 384 - 396, **1979**.

[6] M. Heß, *Aufwertung bei Axialventilatoren - Einfluss von Reynolds-Zahl, Rauheit, Spalt und Betriebspunkt auf Wirkungsgrad und Druckziffer*, Technische Universität Darmstadt, **2010**.

[7] S. S. Stonjek, *Einfluss der Reynolds- und Machzahl auf die Aufwertungsmethodik für Radialventilatoren*, Abschlussbericht Nr. L240 für die Forschungsvereinigung für Luft- und Trocknungstechnik. FLT., Frankfurt a. M., **2014**.

[8] S. Saul, *Belastbare Validierung und Erweiterung einer Aufwertungsmethodik für Radialventialventilatoren*, Abschlussbericht Nr. L243 für die Forschungsvereinigung für Luft- und Trochnungstechnik (FLT), Frankfurt a. M., **2017**.

[9] P. Pelz and S. Stonjek, *A Second Order Exact Scaling Method for Turbomachinery Performance Prediction*, in International Journal of Fluid Machinery and Systems, **2013**.

[10] J. N. Newman, *Marine Hydrodynamics*, Cambridge, Massachusetts, USA: MIT Press, **1977**.

[11] J. F. Gülich, *Kreiselpumpen - Handbuch für Entwicklung, Anlagenplanung und Betrieb*, Springer, **2010**.

[12] D. Thoma, *Der "Stossverlust" des Wassers beim Eintritt in Schaufelsysteme*, Schweizische Bauzeitung, p. 83, **1922**.

[13] S. Saul, S. Stonjek und P. Pelz, *Influence of Compressibility on Incidence Losses of Turbomachinery at Subsonic Operation*, FAN 2015, France, **2015**.

[14] T. Carolus, *Ventilatoren - Aerodynamischer Entwurf, Schallvorhersage, Konstruktion*, Wiesbaden: Springer Vieweg, **2013**.

[15] S. Lieblein, *Experimental flow in two-dimensional cascades*, in Aerodynamic design of axial-flow compressors, Washington, National Aeronautics and Space Administration, pp. 183-226, **1965**.

[16] S. Saul, *Validierung der Darmstädter Aufwerteformel für Axialventilatoren mit dem Nabenverhältnis von 0.625 Ergänzung – FLT-Eigenmittelvorhaben L231*, Abschlussbericht Nr. L259 für die Forschungsvereinigung für Luft- und Trocknungstechnik (FLT), Frankfurt a. M., **2017**.

[17] DIN 24163 (Teil 1-3), *Ventilator - Leistungsmessung, Normkennlinien / Deutsches Institut für Normung (DIN)*, DIN, **1985**.